

FIG. 2. Sampling frequency as function of bar orientation with respect to square matrix.

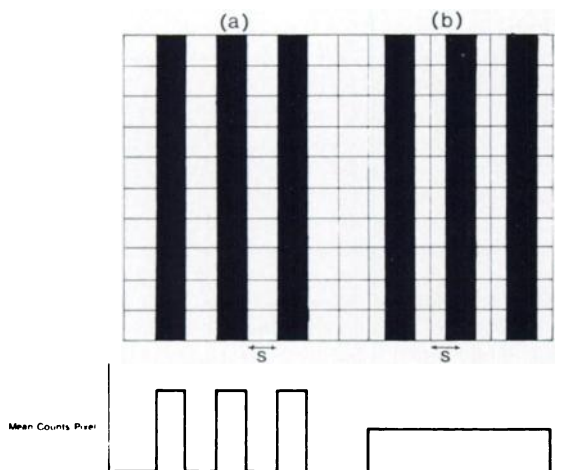


FIG. 3. Variation of contrast as function of bar displacement with respect to square matrix. (A) Bar pattern aligned with matrix: 100% contrast. (b) Bar pattern displaced by $\frac{1}{2}$ pixel width: 0% contrast.

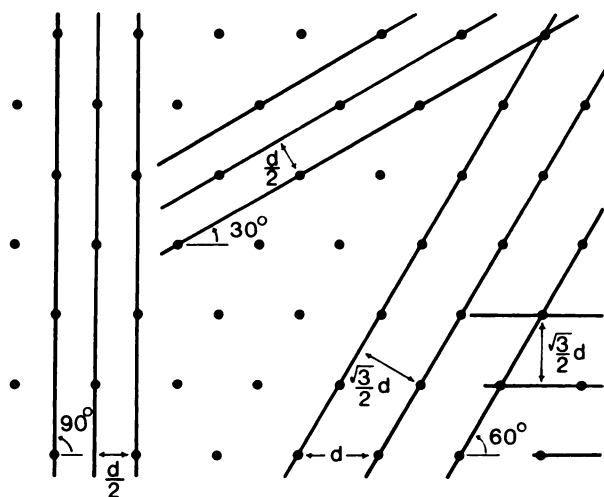


FIG. 4. Sampling frequency in hexagonal matrix as a function of bar orientation.

orientations should have bars and spaces of one-half the hole-separation distance. When the bars are aligned at 0 and 60° to the

septa, the finest bars discernible should be of the order of $\sqrt{3}/2$ of the hole-separation distance. Therefore, for equivalent hole-separation distance and pixel size in the collimator and the computer matrix respectively, the collimator is capable of superior bar-pattern resolution due to the hexagonal configuration of the array.

A comprehensive review of the effects of two-dimensional image sampling, including a discussion of the moiré fringe effect, is given by Legault (4).

DOUGLAS R. SHEARER
 ROLAND WONG
 Rhode Island Hospital
 Providence, Rhode Island

REFERENCES

1. YEH E-L: Distortion of bar-phantom image by collimator. *J Nucl Med* 20: 260-261, 1979
2. BONTE FJ, GRAHAM KD, DOWDEY JE: Image aberrations produced by multichannel collimators for a scintillation camera. *Radiology* 98: 329-334, 1971
3. BONTE FJ, DOWDEY JE: Further observations on the septum effect produced by multichannel collimators for a scintillation camera. *Radiology* 102: 653-656, 1972
4. LEGAULT R: The aliasing problems in two-dimensional sampled imagery. In *Perception of Displayed Information*, Biberman LM, ed. New York, Plenum Press, 1973, pp 279-312

Distortion of Bar Phantom Images Due to Image Digitalization

The point made by the above paper is well taken, but further amplification of certain points may be in order.

The Nyquist sampling theorem (1), which is the basis of modern communication theory, states that in order to completely characterize a waveform that contains a maximum frequency component of f_m (cycles/mm), it is necessary to take at least $2f_m$ (cycles/mm) samples. If fewer samples than this are taken, "aliasing" may occur in which high frequency components appear as erroneous low frequency components. Aliasing results in permanent distortion of the data that cannot be removed by later processing. This fact may be demonstrated by the images shown in the above paper (2).

If we first pay attention to the case in which the bar phantom is oriented at right angles to the coordinates of the data matrices (Fig. 1: Da, Db, and Dc), we first note that the sampling intervals are said to be 2, 4, and 8 mm, respectively, for 128×128 , 64×64 , and 32×32 element data matrices. The bar phantom images may be viewed in cross section as a train of square waves. Fourier analysis of such a waveform would show a basic spatial frequency of 0.125 cy/mm for the 4-mm wide bars. Based on the assumption that the frequency response described by the modulation transfer function of the gamma camera limits the frequency content of the resulting image to about 0.25 cycle/mm, the Nyquist theorem would require a sampling interval of no larger than 2 mm for the quadrant containing the 4-mm bars.

We see then that the 128×128 matrix should properly digitize and display frequency components at least as high as the second spatial harmonic of the 4-mm bars whereas the 64×64 matrix will do this for the 9.5 mm bars only. The 32×32 matrix will be capable of digitizing only the basic frequency of the 9.5-mm quadrant. These facts suggest that errors due to aliasing may very well occur in all quadrants of the 32×32 image and in all but the 9.5-mm quadrant of the 64×64 image.

If the phantom is oriented at 45° to the coordinates of the sampling matrix (Fig. 1: Ba, Bb, and Bc), the sample intervals are

reduced by a factor of $1/\sqrt{2}$ as described by Shearer, and now will properly sample waveforms whose periods are 2.8, 5.6, and 11.2 mm, respectively. This suggests that the 6.4-mm bars will be imaged better, since the second spatial harmonic is now properly sampled but that little or no reduction in artifact may be expected in either the 32×32 matrix or in the remaining quadrants of the 64×64 matrix.

In conclusion, the sampling interval and coarseness of collimation chosen for digitizing an image should be based on a knowledge of the spatial frequency content of the object being imaged. Failure to properly sample the data will result in artifacts that may not be removed later.

CHARLES M. KRONENWETTER
EN-LIN YEH
VA Medical Center
Wood, Wisconsin

REFERENCES

1. SCHWARTZ, M: *Information Transmission, Modulation, and Noise*. New York, McGraw Hill, 1959, pp 169-172
2. SHEARER DR, WONG R: Distortion of bar phantom images as a result of two-dimensional sampling. *J Nucl Med* 20: 1315-1316, 1979

Calculation of Radioactive Decay with a Pocket Calculator

A short letter under the above title by James S. Robertson (1) prompts me to remark that much more sophisticated calculations can be made with only a few steps on a programmable pocket calculator (e.g., HP 25). The decay of a simple radioactive substance can be modeled by the discrete time analogue (Fig. 1) in which the value of the multiplier a is just $\exp(-\lambda\tau)$, τ being any convenient unit time interval. To take the simplest case, if the numbers 0, 0, 1, 0, 0, 0, ... are used as the input sequence $\{x\}$, the output sequence $\{y\}$ will be the numbers 0, 0, 1, $\exp(-\lambda\tau)$, $\exp(-2\lambda\tau)$, $\exp(-3\lambda\tau)$... and these represent the activity at successive intervals, τ , generated by a single unit activity. To realize the model for say Tc-99m (half-life 6.05 hr) it would be appropriate to calculate $\exp(-0.6932/6.05)$ and enter this result into STO 1. The following program should be keyed in:

01	$x \geq y$
02	RCL 1
03	x
04	+
05	GTO 00

To use the program, all that has to be done is to enter a sequence of numbers (starting with a zero), alternating with the R/S command. Step 01 in the program inserts a newly entered x value into the Y register, transferring the previous output into the X register. Step 02 recalls the contents of Store 1, i.e., $\exp(-0.6932/6.05)$, and step 03 multiplies this by the contents of the X register. Step 04 adds on the contents of the Y register. Step 05 halts the calculator with the total displayed in the X register, and the calculator is then ready to receive the next input. Each cycle therefore introduces a multiplication by the exponential factor and an addition of a new input. The displays then show the activity accumulated at 1-hr intervals.

The advantage of the technique is that it enables one to calculate the amount of activity available not only from a single initial source of any strength, but also from any arbitrary set of sources generated at intervals, such as might be produced from a reactor or other machine, or from decay of a parent source.

For a radionuclide with decay constant λ_2 , generated from a

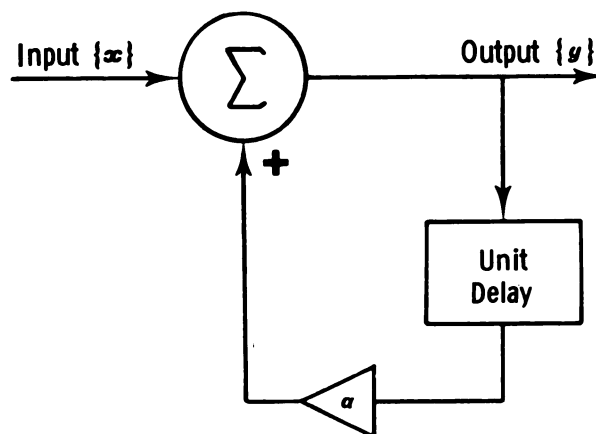


FIG. 1. One-component discrete time analogue.

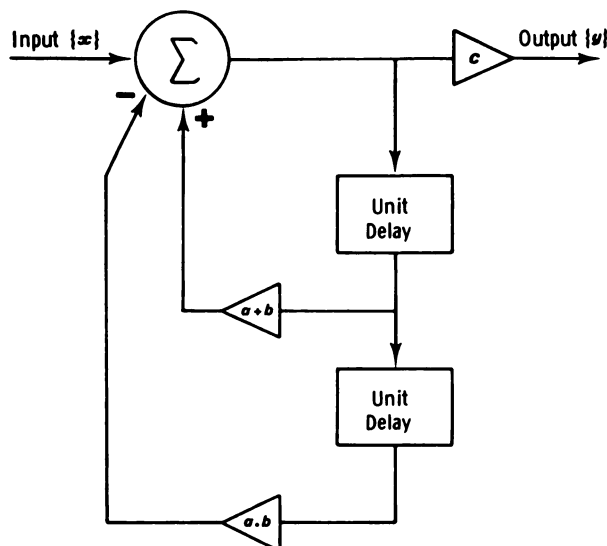


FIG. 2. Two-component discrete time analogue.

parent with decay constant λ_1 a model such as that of Fig. 2 can be used.

In this the factors a , b , c are given by $a = \exp(-\lambda_1)$, $b = \exp(-\lambda_2)$, $c = t_1(a - b)/(t_1 - t_2)$, where t_1 , t_2 are the respective half-lives.

A program for an HP 25 calculator based on this model occupies about 27 steps. (Copies will be sent to anyone interested.) The program is operated in the same way as the one-component program, allowing convolutions to be performed with any arbitrary input sequence. If the input sequence represents parent activity in any unit (e.g., mCi), the output will give the daughter activity in the same unit.

K. F. CHACKETT
Dudley Road Hospital
Birmingham, England

REFERENCE

1. ROBERTSON, JS: Calculation of radioactive decay with a pocket calculator. *J Nucl Med* 19: 1270-1271, 1978